

Beating the Efficiency of Both Quantum and Classical Simulations with a Semiclassical Method

Cesare Mollica and Jiří Vaníček*

Laboratory of Theoretical Physical Chemistry, Institut des Sciences et Ingénierie Chimiques,
Ecole Polytechnique Fédérale de Lausanne, Lausanne, Switzerland

(Received 18 August 2011; published 14 November 2011)

While rigorous quantum dynamical simulations of many-body systems are extremely difficult (or impossible) due to exponential scaling with dimensionality, the corresponding classical simulations ignore quantum effects. Semiclassical methods are generally more efficient but less accurate than quantum methods and more accurate but less efficient than classical methods. We find a remarkable exception to this rule by showing that a semiclassical method can be both more accurate and faster than a classical simulation. Specifically, we prove that for the semiclassical dephasing representation the number of trajectories needed to simulate quantum fidelity is independent of dimensionality and also that this semiclassical method is even faster than the most efficient corresponding classical algorithm. Analytical results are confirmed with simulations of fidelity in up to 100 dimensions with 2^{1700} -dimensional Hilbert space.

DOI: [10.1103/PhysRevLett.107.214101](https://doi.org/10.1103/PhysRevLett.107.214101)

PACS numbers: 05.45.Mt, 03.65.Sq, 05.45.Jn, 05.45.Pq

Introduction.—A correct description of many microscopic dynamical phenomena, such as ultrafast time-resolved spectra or tunneling rate constants, requires an accurate quantum (QM) simulation. While classical (CL) molecular dynamics simulations are feasible for millions of atoms, the solution of the time-dependent Schrödinger equation scales exponentially with the number D of degrees of freedom (DOF) and is feasible for only a few continuous DOF. An apparently promising solution is provided by semiclassical (SC) methods, which use CL trajectories but attach to them phase information and thus can approximately describe interference and other QM effects completely missed in CL simulations. Unfortunately, SC methods suffer from the “dynamical sign problem” due to the addition of rapidly oscillating terms, resulting in the requirement of a huge number of CL trajectories for convergence. Consequently, most SC methods are much less efficient than CL simulations and in practice were used for at most tens of DOF. Even though several techniques have explored this issue [1], the challenge remains open. Below, we turn this challenge around by showing that in simulations of QM fidelity (QF) [2,3], a SC method called “dephasing representation” (DR) [4–6] is not only more accurate but, remarkably, also *faster* than the most efficient corresponding CL algorithm [7].

Quantum fidelity.—QF was introduced by Peres [8] to measure the stability of QM dynamics (QD). He defined QF $F^{\text{QM}}(t)$ as the squared overlap at time t of two QM states, identical at $t = 0$, but subsequently evolved with two different Hamiltonians H_0 and $H_\epsilon = H_0 + \epsilon V$:

$$F^{\text{QM}}(t) := |f^{\text{QM}}(t)|^2, \quad (1)$$

$$f^{\text{QM}}(t) := \langle \psi | U_\epsilon^{-t} U_0^t | \psi \rangle, \quad (2)$$

where $f^{\text{QM}}(t)$ is the fidelity amplitude and $U_\epsilon^t := \exp(-iH_\epsilon t/\hbar)$ the QM evolution operator. By rewriting

Eq. (2) as $f^{\text{QM}}(t) = \langle \psi | U^t | \psi \rangle$ with the echo operator $U^t := U_\epsilon^{-t} U_0^t$, it can be interpreted as the Loschmidt echo, i.e., an overlap of an initial state with a state evolved for time t with H_0 and subsequently for time $-t$ with H_ϵ . (In general, we write time t as a superscript. Subscript ϵ denotes that H_ϵ was used for dynamics. If an evolution operator, phase-space coordinate, or density lacks a subscript ϵ , Loschmidt echo dynamics is implied.) QF appears, e.g., in NMR spin echo experiments [9], neutron scattering [10], ultrafast electronic spectroscopy [11,12], and QM computation and decoherence [13]. QF can be also used to measure nonadiabaticity [14] or accuracy of molecular QD on an approximate potential energy surface [15].

Classical fidelity.—Assuming for simplicity that the initial states are pure, one may write QF (1) as $F^{\text{QM}}(t) = \text{Tr}(\hat{\rho}_\epsilon^t \hat{\rho}_0^t)$, where $\hat{\rho}_\epsilon^t := U_\epsilon^t \hat{\rho} U_\epsilon^{-t}$ is the density operator at time t . In the phase-space formulation of QM mechanics, $F^{\text{QM}}(t) = h^{-D} \int dx \rho_\epsilon^{\text{W},t}(x) \rho_0^{\text{W},t}(x)$, where $x := (q, p)$ is a point in phase space and $A^{\text{W}}(x) := \int d\xi \langle q - \xi/2 | \hat{A} | q + \xi/2 \rangle e^{ip\xi/\hbar}$ the Wigner transform of \hat{A} . This form of QF suggests its CL limit, called CL fidelity (CF) [16,17]:

$$F^{\text{CL}}(t) := h^{-D} \int dx \rho_\epsilon^{\text{CL},t}(x) \rho_0^{\text{CL},t}(x) \quad (3)$$

$$= h^{-D} \int dx \rho^{\text{CL},t}(x) \rho^{\text{CL},0}(x), \quad (4)$$

where the two lines express CF in the fidelity and Loschmidt echo pictures, respectively. From now on, if ρ lacks superscript “W,” then “CL” is implied.

Semiclassical dephasing representation.—In order to capture the QM effects missing in CF, several methods were proposed to describe QF semiclassically. Most were analytical [3,18] and valid only under special circumstances because the numerical approaches were

overwhelmed with the sign problem. By extending a numerically practical SC method for localized Gaussian wave packets (GWPs) [19], the SC DR was introduced as a more accurate and general SC approximation of QF [4–6]. The DR of QF is defined as $F^{\text{DR}} := |f^{\text{DR}}|^2$, where the DR amplitude is an interference integral:

$$f^{\text{DR}}(t) := h^{-D} \int dx^0 \rho^{\text{W}}(x^0) \exp[i\phi(x^0, t)], \quad (5)$$

$$\phi(x^0, t) := -\Delta S(x^0, t)/\hbar = (\epsilon/\hbar) \int_0^t d\tau V(x_{\epsilon/2}^{\tau}), \quad (6)$$

and phase ϕ is determined by the action ΔS due to the perturbation along a trajectory propagated with the average Hamiltonian $H_{\epsilon/2}$ [12,20]. Above, $x_{\epsilon}^t := \Phi_{\epsilon}^t(x^0)$, where Φ_{ϵ}^t is the Hamiltonian flow of H_{ϵ} . The DR was successfully used to describe stability of QD in integrable, mixed, and chaotic systems [4–6], nonadiabaticity [14] and accuracy of molecular QD on an approximate potential energy surface [15], and the local density of states and the transition from the Fermi golden rule (FGR) to the Lyapunov regime of QF decay [21]. The same approximation was independently derived and used in electronic spectroscopy [11]. Recently, the DR was derived from the SC theory of Wigner function evolution and its range of validity extended with a SC amplitude correction [20].

The remarkable efficiency of the original implementation of DR observed empirically in applications led us to analyze this property rigorously here. Figure 1, displaying fidelity in a 100-dimensional system (see the section on numerical results for details), advertises the main result to be proven analytically below. The figure shows that algorithms *deph-1* for F^{DR} and recently proposed [7] *echo-2* for F^{CL} converge with several orders of magnitude fewer trajectories than previously used algorithms for F^{CL} , but, while the DR reproduces the plateau of F^{QM} , even the fully converged CF (computed as a product of 100 one-dimensional fidelities) does not capture this QM effect.

Algorithms.—The most general and straightforward way to evaluate Eqs. (3)–(5) is with trajectory-based methods. While the DR (5) is already in a suitable form, Eqs. (3) and (4) for CF must be rewritten by using the Liouville theorem as

$$F^{\text{CL}}(t) = h^{-D} \int dx^0 \rho(x_{\epsilon}^{-t}) \rho(x_0^{-t}) \quad (7)$$

$$= h^{-D} \int dx^0 \rho(x^{-t}) \rho(x^0). \quad (8)$$

Above, $x^t := \Phi^t(x^0)$, where $\Phi^t := \Phi_{\epsilon}^{-t} \circ \Phi_0^t$ is the Loschmidt echo flow. Since it is the phase-space points rather than the densities that evolve in expressions (7) and (8), we can take $\rho = \rho^{\text{W}, t=0}$. For numerical computations, Eqs. (5), (7), and (8) are further rewritten in a form suitable for Monte Carlo evaluation, i.e., as an average

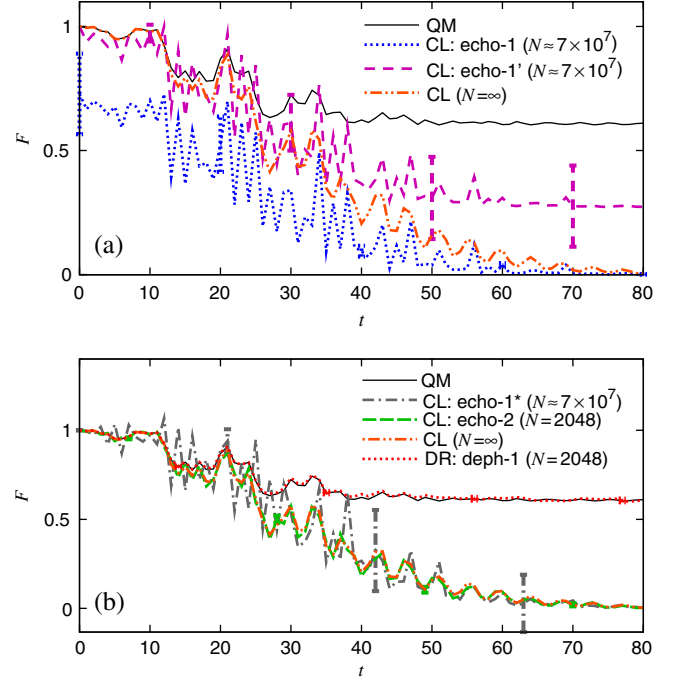


FIG. 1 (color online). Convergence of different fidelity algorithms in a 100-dimensional system of perturbed ($\epsilon = 3 \times 10^{-4}$) quasi-integrable ($k = 0.2$) kicked rotors with $n_1 = 8192$ for an initial GWP with $X = (0.7, 0.24) \times 2\pi$ and $a = \sqrt{\hbar}$ in all dimensions. Error bars are plotted every 20 time steps. (a) Simple algorithms *echo-1* and *echo-1'* are far from converged even with 7×10^7 trajectories. (b) While both $F_{\text{deph-1}}^{\text{DR}}$ and $F_{\text{echo-2}}^{\text{CL}}$ converge fully with only 2048 trajectories, only the DR can capture the QM fidelity “freeze” (the plateau).

$$\langle A(x^0, t) \rangle_{W(x^0)} := \frac{\int dx^0 A(x^0, t) W(x^0)}{\int dx^0 W(x^0)},$$

where W is the sampling weight for initial conditions x^0 . While previously used CL algorithms sampled from $W = \rho$ [17,22], Ref. [7] considered more general weights $W = W_M(x^0) := \rho(x^0)^M$ and $W = W_M(x_0^{-t}) = \rho[\Phi_0^{-t}(x^0)]^M$ for the echo and fidelity dynamics, respectively. These weights yield four families of M -dependent algorithms [7]:

$$F_{\text{fid-}M}^{\text{CL}}(t) = I_M \langle \rho(x_{\epsilon}^{-t}) \rho(x_0^{-t})^{1-M} \rangle_{\rho(x_0^{-t})^M}, \quad (9)$$

$$F_{\text{echo-}M}^{\text{CL}}(t) = I_M \langle \rho(x^{-t}) \rho(x^0)^{1-M} \rangle_{\rho(x^0)^M}, \quad (10)$$

$$F_{\text{fid-}M^*}^{\text{CL}}(t) = \frac{\langle \rho(x_{\epsilon}^{-t}) \rho(x_0^{-t})^{1-M} \rangle_{\rho(x_0^{-t})^M}}{\langle \rho(x_0^{-t})^{2-M} \rangle_{\rho(x_0^{-t})^M}}, \quad (11)$$

$$F_{\text{echo-}M^*}^{\text{CL}}(t) = \frac{\langle \rho(x^{-t}) \rho(x^0)^{1-M} \rangle_{\rho(x^0)^M}}{\langle \rho(x^0)^{2-M} \rangle_{\rho(x^0)^M}}, \quad (12)$$

where $I_M := h^{-D} \int \rho(x^0)^M dx^0$ is a normalization factor. Conveniently, the “normalized” (*) algorithms (11) and (12) do not require the normalization factor I_M which is,

for general states, known explicitly only for $M \in \{0, 1, 2\}$ ($I_0 = n_1^D$, $I_1 = I_2 = 1$). For further details, see Ref. [7], where it was found that the echo-2 algorithm is optimal since it is already normalized (i.e., echo-2 = echo-2*), applies to any density (in particular, ρ does not have to be positive definite), and—most importantly—is by far the most efficient CL algorithm.

As for the DR amplitude, one does not need to consider general values of M since taking $M = 1$, i.e., $W = \rho^W(x^0)$, already gives the desired efficient algorithm deph-1 [4–6]:

$$f_{\text{deph-1}}^{\text{DR}}(t) = \langle \exp[i\phi(x^0, t)] \rangle_{\rho^W(x^0)}. \quad (13)$$

Sampling is straightforward for $\rho^W \geq 0$ but can be done also for general states with nonpositive definite ρ^W [6].

Efficiency.—The reader does not have to be persuaded of the exponential scaling of QD with D . We just note that the direct diagonalization of the Hamiltonian leads to a QD algorithm with a cost $O(t^0 n_D^3) = O(t^0 n_1^{3D})$, where $n_D = n_1^D$ is the dimension of the Hilbert space of D DOF. Despite the independence of t , the scaling with D is overwhelming. More practical is the split-operator algorithm requiring the fast Fourier transform at each step. The complexity of the fast Fourier transform is $O(n_D \log n_D)$; hence, the overall cost is $O(t D n_1^D \log n_1)$. The effective n_1 is reduced in increasingly popular methods with evolving bases, but the exponential scaling remains.

Regarding the algorithms for CF and DR, the efficiency of trajectory-based methods depends on two ingredients: First, what is the cost of propagating N trajectories for time t ? Second, what N is needed to converge the result to within a desired discretization error σ_{discr} ? As this analysis was done for the CL algorithms in Ref. [7], here we only outline the main ideas and apply them to analyze the efficiency of the DR.

The cost of a typical method propagating N trajectories for time t is $O(c_f t N)$, where c_f is the cost of a single force evaluation. However, among the above mentioned algorithms, this is true only for the fidelity algorithms with $M = 0$ (i.e., fid-0 and fid-0*) and for the DR. Remarkably, in all other cases, the cost is $O(c_f t^2 N)$. The cost is linear in time for a single time t but becomes quadratic if one wants to know CF for all times up to t . For the echo algorithms, it is due to the necessity of full backward propagation for each time between 0 and t . For the fidelity algorithms, it is because the weight function $\rho(x^{-t})^M$ changes with time and the sampling has to be redone for each time between 0 and t [7].

The number N of trajectories required for convergence can depend on D , t , the dynamics, the initial state, and the method. Below, we estimate N for the DR analytically by using the technique proposed in Ref. [7]. The discretization error of $A(N)$ due to finite N is computed as $\sigma_{A, \text{discr}}^2(N) := \overline{|A(N) - A|^2}$, where the overline denotes an average over infinitely many independent simulations with N trajectories. The expected systematic component of σ_{discr} is zero

for $f_{\text{deph-1}}^{\text{DR}}$ and $O(N^{-1})$ for $F_{\text{deph-1}}^{\text{DR}}$ and is negligible to the expected statistical component $\sigma = O(N^{-1/2})$, which therefore determines convergence. The expected statistical error of $A(N)$ is computed as $\sigma_A^2(N) = \overline{|A(N)|^2} - |\overline{A(N)}|^2$.

The discretized form of Eq. (13) is $f_{\text{deph-1}}^{\text{DR}}(t, N) = N^{-1} \sum_{j=1}^N \exp[i\phi(x_j^0, t)]$, from which $|\overline{f_{\text{deph-1}}^{\text{DR}}(t, N)}|^2 = N^{-1} + (1 - N^{-1})F^{\text{DR}}(t)$, $|\overline{f_{\text{deph-1}}^{\text{DR}}(t, N)}|^2 = F^{\text{DR}}(t)$, and $\sigma_{f_{\text{deph-1}}^{\text{DR}}}^2 = N^{-1}[1 - F^{\text{DR}}(t)]$. The analogous calculation for $F_{\text{deph-1}}^{\text{DR}}$ is somewhat more involved but straightforward. Inverting the results for $\sigma_{f_{\text{deph-1}}^{\text{DR}}}^2$ (exactly) and $\sigma_{F_{\text{deph-1}}^{\text{DR}}}^2$ (to leading order in N) gives

$$N_{f_{\text{deph-1}}^{\text{DR}}} = \sigma^{-2}(1 - F^{\text{DR}}) \quad \text{and} \quad (14)$$

$$N_{F_{\text{deph-1}}^{\text{DR}}} = \frac{2}{\sigma^2} [\text{Re}(\langle e^{i2\phi} \rangle_{\rho^W} \langle e^{-i\phi} \rangle_{\rho^W}^2) + F^{\text{DR}} - 2(F^{\text{DR}})^2]. \quad (15)$$

Result (14) for $N_{f_{\text{deph-1}}^{\text{DR}}}$ is completely general. As for $N_{F_{\text{deph-1}}^{\text{DR}}}$, using the inequality $|\langle e^{i2\phi} \rangle_{\rho^W(x^0)}| \leq 1$ and Eq. (13), we can find a completely general upper bound:

$$N_{F_{\text{deph-1}}^{\text{DR}}} \leq 4\sigma^{-2} F^{\text{DR}}(1 - F^{\text{DR}}). \quad (16)$$

Estimate (14) and upper bound (16) show, remarkably, that without any assumptions the numbers of trajectories needed for convergence of both $f_{\text{deph-1}}^{\text{DR}}$ and $F_{\text{deph-1}}^{\text{DR}}$ depend only on σ and F^{DR} and are *independent* of D , t , initial state, or dynamics. Estimate (15) of $N_{F_{\text{deph-1}}^{\text{DR}}}$ can be evaluated analytically for normally distributed phase ϕ . This is satisfied very accurately in the chaotic FGR and integrable Gaussian regimes [2,3] and exactly for pure displacement dynamics of GWPs. By noting that for normal distributions $\langle e^{i\phi} \rangle = e^{i\langle \phi \rangle} \exp[-\text{Var}(\phi)/2]$ and $F^{\text{DR}} = |f_{\text{deph-1}}^{\text{DR}}|^2 = \exp[-\text{Var}(\phi)]$, Eq. (15) reduces to

$$N_{F_{\text{deph-1}}^{\text{DR}}, \text{normal}} = 2\sigma^{-2} F^{\text{DR}}(1 - F^{\text{DR}})^2, \quad (17)$$

which is again *independent* of D , t , the initial state, or the dynamics.

In Ref. [7], it was found with a similar analysis that, for CF algorithms (9)–(12) and $D \gg 1$, one needs $N = \sigma^{-2} \alpha(F) \beta^D$ trajectories, where α and β depend on the method, initial state, and dynamics. For all methods with $M \neq 2$, there are simple examples [7] with $\beta > 1$, implying an exponential growth of N with D . Remarkably, for any dynamics and any initial state, $N = \sigma^{-2}[1 - (F^{\text{CL}})^2]$ for the echo-2 algorithm, so $\beta = 1$ and, as for the DR, N is independent of D [7].

Numerical results and conclusion.—To illustrate the analytical results, numerical tests were performed in D -dimensional systems of uncoupled displaced simple harmonic oscillators (SHOs, for pure displacement dynamics) with $H = p^2/2 + k(q \pm \Delta q)^2/2$ and perturbed kicked

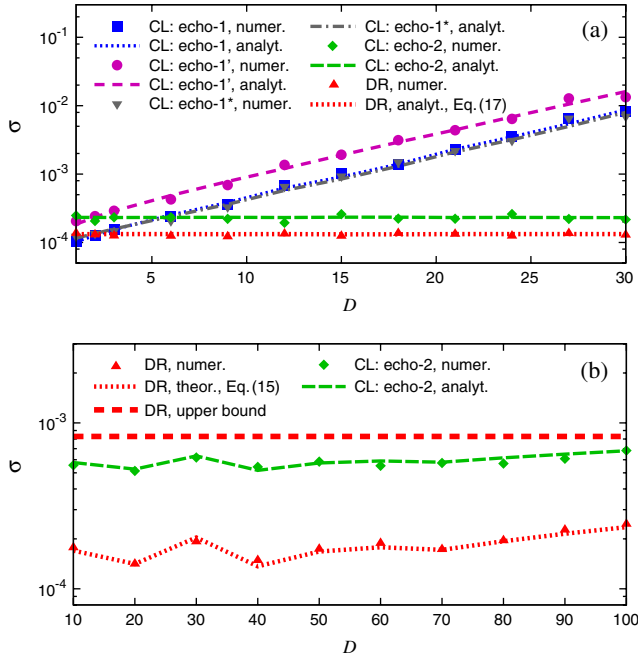


FIG. 2 (color online). Statistical error grows exponentially with D for the echo-1, echo-1', and echo-1* algorithms, while it is independent of D for the CL echo-2 algorithm and the DR (computed always with the depth-1 algorithm). (a) Pure displacement dynamics obtained with two displaced D -dimensional SHOs. $N \approx 10^7$. Times were chosen separately for each D so that $F \approx 0.3$. (b) General dynamics obtained with a D -dimensional system of perturbed ($\epsilon = 10^{-4}$) quasi-integrable ($k = 0.2$) kicked rotors with $n_1 = 131\,072$. $N \approx 5 \times 10^5$. Times were chosen separately for each D so that $F \approx 0.9$.

rotors (for nonlinear integrable and chaotic dynamics). The last model is defined, $\text{mod}(2\pi)$, by the map $q_{j+1} = q_j + p_j$, $p_{j+1} = p_j - \nabla W(q_{j+1}) - \epsilon \nabla V(q_{j+1})$, where $W(q) = -k \cos q$ and $V(q) = -\cos(2q)$; k and ϵ

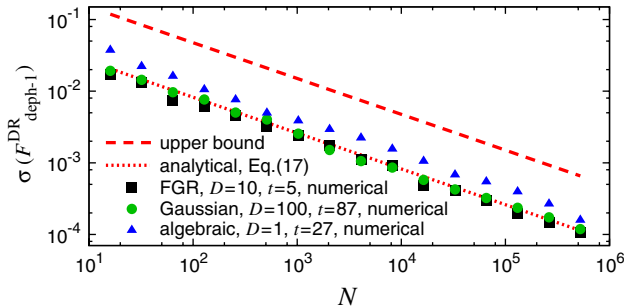


FIG. 3 (color online). Regardless of dynamics, the statistical error of the DR is independent of dimensionality (D) and time (t) and is proportional to $N^{-1/2}$. Errors are compared for 10 kicked rotors in the chaotic FGR regime ($k = 18$, $\epsilon = 6.4 \times 10^{-6}$, $n_1 = 131\,072$), 100 kicked rotors in the integrable Gaussian regime ($k = 0.2$, $\epsilon = 6.4 \times 10^{-6}$, $n_1 = 131\,072$), and a single kicked rotor in the quasi-integrable algebraic regime ($k = 0.2$, $\epsilon = 6.4 \times 10^{-4}$, $n_1 = 131\,072$). Time t was chosen separately for each system so that $F \approx 0.94$.

determine the type of dynamics and perturbation strength, respectively. Uncoupled systems were used to make QF calculations feasible (as a product of D one-dimensional calculations); however, both CF and DR calculations were performed as for a truly D -dimensional system. The initial state was always a D -dimensional GWP $\rho^W(x) := 2^D \exp[-(q - Q)^2/a^2 - (p - P)^2/a^2/\hbar^2]$. Expected statistical errors were estimated by averaging actual statistical errors over 100 different sets of N trajectories, and no fitting was used in any of the figures. Note that results are also shown for algorithm echo-1', $F_{\text{echo-1}'}^{\text{CL}}(t) = 1 + \langle \rho(x^{-t}) - \rho(x^0) \rangle_{\rho(x^0)}$, a variant of echo-1 precise for high fidelity [7].

Figure 2 confirms that, whereas the statistical errors of echo-1, echo-1', and echo-1* algorithms grow exponentially with D , the statistical errors of the $F_{\text{depth-1}}^{\text{DR}}$ and $F_{\text{echo-2}}^{\text{CL}}$ are independent of D . Figure 3 shows that, for several very different dynamical regimes, $\sigma_{F_{\text{depth-1}}^{\text{DR}}}$ is independent of t , D , and n_1 , in agreement with the general upper bound (16) and—in the FGR and Gaussian regimes—also in agreement with the analytical estimate (17). Figure 4 exhibits

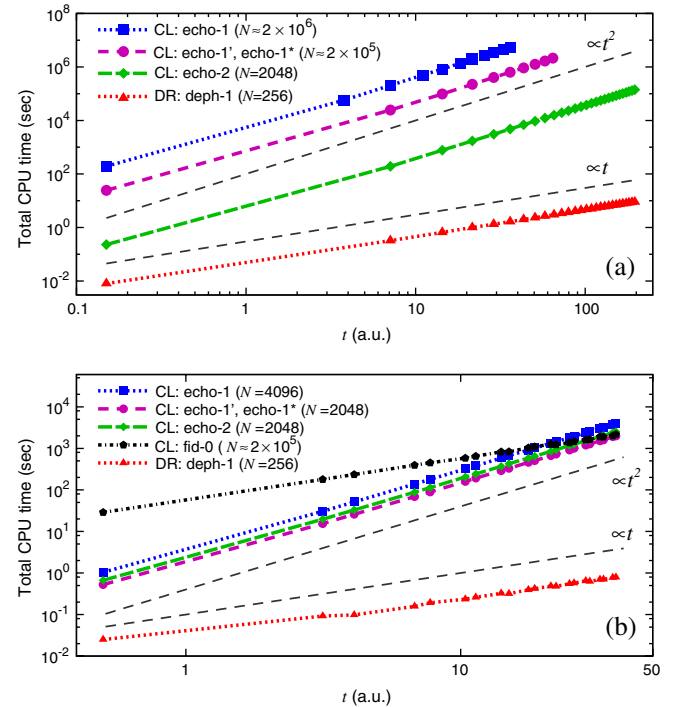


FIG. 4 (color online). Computational cost as a function of simulation time t grows quadratically for all CL echo algorithms while it is only linear for the DR:depth-0 and CL:fid-0 algorithms. Pure displacement dynamics is given by two D -dimensional displaced SHOs ($k = 3$ and $\hbar = 1$) for which all algorithms converge to the exact result. The initial GWP had $X = (0.5, 1)$ and $a = 1$ in all DOFs. The fidelity was computed at fidelity revival times at which $F \approx 0.9$. The number of trajectories (N) was selected for each algorithm separately so that the statistical error $\sigma \approx 0.01$. (a) $D = 20$, $\Delta q = 0.2$. (b) $D = 1$, $\Delta q = 0.35$.

the superior overall efficiency of the DR compared to all CF algorithms: Thanks to linear scaling with t and independence of D , the DR is orders of magnitude faster already for quite a small system and short time.

In conclusion, in the case of QF, a SC method can be not only more accurate but also more efficient than a CL simulation of QD. In particular, the number of trajectories needed for convergence of the SC DR depends on F but not on D , t , the initial state, or the type of dynamics as naïvely expected. This counterintuitive result should be useful for future development of approximate methods for QD of large systems.

This research was supported by Swiss NSF Grant No. 200021_124936 and NCCR MUST and by EPFL. We thank E. Heller, T. Seligman, M. Šulc, and T. Zimmermann for discussions.

*jiri.vanicek@epfl.ch

- [1] A. R. Walton and D. E. Manolopoulos, *Mol. Phys.* **87**, 961 (1996); K. G. Kay, *J. Chem. Phys.* **101**, 2250 (1994); T. Sklarz and K. G. Kay, *ibid.* **120**, 2606 (2004); H. Wang, X. Sun, and W. H. Miller, *ibid.* **108**, 9726 (1998); J. Tatchen, E. Pollak, G. Tao, and W. H. Miller, *ibid.* **134**, 134104 (2011); G. Tao and W. H. Miller, *ibid.* **135**, 024104 (2011); J. Vaníček and E. J. Heller, *Phys. Rev. E* **64**, 026215 (2001); **67**, 016211 (2003).
- [2] T. Gorin, T. Prosen, T. H. Seligman, and M. Žnidarič, *Phys. Rep.* **435**, 33 (2006).
- [3] P. Jacquod and C. Petitjean, *Adv. Phys.* **58**, 67 (2009).
- [4] J. Vaníček, *Phys. Rev. E* **70**, 055201 (2004).
- [5] J. Vaníček, [arXiv:quant-ph/0410205](https://arxiv.org/abs/quant-ph/0410205).
- [6] J. Vaníček, *Phys. Rev. E* **73**, 046204 (2006).
- [7] C. Mollica, T. Zimmermann, and J. Vaníček, [arXiv:1108.0173](https://arxiv.org/abs/1108.0173).
- [8] A. Peres, *Phys. Rev. A* **30**, 1610 (1984).
- [9] H. M. Pastawski, P. R. Levstein, G. Usaj, J. Raya, and J. Hirschinger, *Physica (Amsterdam)* **283A**, 166 (2000).
- [10] C. Petitjean, D. V. Bevilaqua, E. J. Heller, and P. Jacquod, *Phys. Rev. Lett.* **98**, 164101 (2007).
- [11] S. Mukamel, *J. Chem. Phys.* **77**, 173 (1982); J. M. Rost, *J. Phys. B* **28**, L601 (1995); Z. Li, J.-Y. Fang, and C. C. Martens, *J. Chem. Phys.* **104**, 6919 (1996); S. A. Egorov, E. Rabani, and B. J. Berne, *ibid.* **108**, 1407 (1998); Q. Shi and E. Geva, *ibid.* **122**, 064506 (2005).
- [12] M. Wehrle, M. Šulc, and J. Vaníček, *Chimia* **65**, 334 (2011).
- [13] F. M. Cucchiatti, D. A. R. Dalvit, J. P. Paz, and W. H. Zurek, *Phys. Rev. Lett.* **91**, 210403 (2003); T. Gorin, T. Prosen, and T. H. Seligman, *New J. Phys.* **6**, 20 (2004).
- [14] T. Zimmermann and J. Vaníček, *J. Chem. Phys.* **132**, 241101 (2010); (unpublished).
- [15] B. Li, C. Mollica, and J. Vaníček, *J. Chem. Phys.* **131**, 041101 (2009); T. Zimmermann, J. Ruppen, B. Li, and J. Vaníček, *Int. J. Quantum Chem.* **110**, 2426 (2010).
- [16] T. Prosen and M. Žnidarič, *J. Phys. A* **35**, 1455 (2002).
- [17] G. Benenti and G. Casati, *Phys. Rev. E* **65**, 066205 (2002).
- [18] R. A. Jalabert and H. M. Pastawski, *Phys. Rev. Lett.* **86**, 2490 (2001); D. Cohen and T. Kottos, *ibid.* **85**, 4839 (2000); N. R. Cerruti and S. Tomsovic, *ibid.* **88**, 054103 (2002).
- [19] J. Vaníček and E. J. Heller, *Phys. Rev. E* **68**, 056208 (2003).
- [20] E. Zambrano and A. M. Ozorio de Almeida, *Phys. Rev. E* **84**, 045201(R) (2011).
- [21] W.-g. Wang, G. Casati, B. Li, and T. Prosen, *Phys. Rev. E* **71**, 037202 (2005); N. Ares and D. A. Wisniacki, *ibid.* **80**, 046216 (2009); D. A. Wisniacki, N. Ares, and E. G. Vergini, *Phys. Rev. Lett.* **104**, 254101 (2010); I. García-Mata, R. O. Vallejos, and D. A. Wisniacki, [arXiv:1106.4206](https://arxiv.org/abs/1106.4206).
- [22] Z. P. Karkuszewski, C. Jarzynski, and W. H. Zurek, *Phys. Rev. Lett.* **89**, 170405 (2002); G. Benenti, G. Casati, and G. Veble, *Phys. Rev. E* **67**, 055202 (2003); **68**, 036212 (2003); G. Veble and T. Prosen, *Phys. Rev. Lett.* **92**, 034101 (2004); G. Casati, T. Prosen, J. Lan, and B. Li, *ibid.* **94**, 114101 (2005); G. Veble and T. Prosen, *Phys. Rev. E* **72**, 025202 (2005).